

Analytical bounds of in-plane Young's modulus and full-field simulations of two-dimensional monocrystalline stochastic honeycomb structures



Duancheng Ma^{a,*}, Philip Eisenlohr^b, Pratheek Shanthraj^{a,c}, Martin Diehl^a, Franz Roters^a, Dierk Raabe^a

^a Max-Planck-Institut für Eisenforschung GmbH, Max-Planck-Straße 1, 40237 Düsseldorf, Germany

^b Chemical Engineering and Materials Science, Michigan State University, East Lansing, 48824 MI, USA

^c Aachen Institute for Advanced Study in Computational Engineering Science, RWTH Aachen University, Schinkelstraße 2, 52062 Aachen, Germany

ARTICLE INFO

Article history:

Received 12 April 2015

Received in revised form 13 July 2015

Accepted 18 July 2015

Available online 1 August 2015

Keywords:

Honeycomb

Cellular material

Anisotropic elasticity

Crystallographic orientation

ABSTRACT

In this study, we focus on the interplay between the honeycomb structure and the crystallographic orientation. Specifically, the in-plane Young's moduli of monocrystalline stochastic honeycombs are calculated by a numerical and an analytical approach. The in-plane Young's moduli of the honeycombs were calculated numerically using a solution scheme for the full-field mechanical equilibrium based on spectral methods and anisotropic crystal elasticity. The analytical approach formulates two alternative assumptions, *i.e.* uniform force and uniform strain per strut, considers the elastic anisotropy of the base material, and depends on the two-variable distribution of the strut length and inclination angle as the structural parameters characterizing the stochastic honeycombs. The uniform strain assumption agrees closely with the numerical simulation results and constitutes an improvement compared to analytical solutions proposed in previous studies.

© 2015 Elsevier B.V. All rights reserved.

1. Introduction

This study is inspired by the recent development and investigations on bulk nanoporous gold (NPG), especially by its applications as actuators and sensors [1–4]. Due to the large length scale difference between the sample size (mm to μm) and the ligament size (nm) [5–7] in addition to the complex cellular structure, the direct observation of the deformation mechanisms of NPG is challenging. Though efforts have been made by using transmission electron microscopy (TEM) and scanning electron microscopy (SEM) [7–11], comprehensive structure–property relations for NPG are still not yet established. Hence, numerical modeling can be an alternative to improve the understanding of the relation between the cellular structure and its mechanical response upon external loading.

To model the elastic response of NPG by means of continuum mechanics, the model morphology needs to be close to the experimental observations, *e.g.* [12–16]. In those previous studies, the constitutive description of the materials is isotropic. As exemplified by Jin *et al.* [7], the mean grain size of NPG is typically orders

of magnitude larger than the ligament size, indicating that an isotropic description might not be adequate to study NPG.

In this study, we explore the interplay between the cellular structure and the elastic anisotropy of the base material. Instead of directly addressing three-dimensional (3D) foams, we focus here on two-dimensional (2D) honeycombs with the aim at studying the orientational dependence of the elastic response of monocrystalline stochastic honeycombs upon in-plane compression. The corresponding study on plastic deformation will be presented and discussed in another publication.

This paper is organized as follows: Section 2 describes the numerical and analytical approaches, the honeycomb structures, and the crystallographic orientation of single crystals considered in this study. Appendix A briefly summarizes the approaches proposed in previous studies [17–19]. Section 3 presents and discusses the results with a summary given in Section 4.

It should be noted that the surface effect is not considered in this study. As observed in atomistic simulations and experiments [20–25], the elastic modulus of a nanowire deviates from that of the bulk material, when the diameter is less than, roughly speaking, 100 nm, depending on the material and the crystallographic orientation. Incorporating surface elasticity into the continuum framework to study nanoporous materials is discussed in [26–33].

* Corresponding author. Tel.: +49 211 6792 330; fax: +49 211 6792 333.

E-mail address: d.ma@mpie.de (D. Ma).

2. Methodology

2.1. Numerical approach

2.1.1. Numerical solver and constitutive law

In this study, we use a spectral method approach to solve the mechanical equilibrium and compatibility conditions as pioneered by Moulinec and Suquet [34]. This solution strategy overcomes the well-known limitations of the finite element method (FEM), such as unfavorable scaling for large problems, the inability to capture high spatial gradients, and the necessity of meshing. Details on the implementation of this method can be found in [35].

We assume anisotropic elastic behavior for single crystalline gold. Non-zero components of its elastic stiffness tensor with cubic symmetry are $C_{11} = 191$ GPa, $C_{12} = 62.0$ GPa, and $C_{44} = 42.2$ GPa [36].

2.1.2. Crystallographic orientations

We selected typical texture components of rolled face-centered cubic (fcc) and body-centered cubic (bcc) crystals as orientations for the single crystalline gold matrix, i.e. 'Brass', 'Copper', 'Cube', 'Goss', 'Rotated Cube', and 'S'. The orientation, termed 'RZ', that is most unstable upon compression in fcc [37] and an arbitrary orientation, termed 'Less symmetric', are additionally considered such that eight different orientations are compared. Table 1 lists details for all selected crystallographic orientations.

2.1.3. Geometry

Each of four stochastic honeycomb structures was generated from 200 randomly positioned seed points by periodic Voronoi tessellation on a 512×512 grid. The grid spacing can be selected arbitrarily since anisotropic elasticity is size independent. A closed-porosity honeycomb with relative density $\rho/\rho_0 \approx 0.6$ is generated by widening all Voronoi cell edges and classifying them as solid phase struts of bulk density ρ_0 while the remaining cell interior is considered void (Fig. 1). No minimum distance between adjacent seed points is enforced in the Voronoi tessellation.

Fig. 2 presents the resulting distributions of strut length and strut inclination angle relative to X axis. As expected for stochastic honeycombs [19] the strut length follows a bimodal distribution.¹ The inclination angle is uniformly (randomly) distributed since any reference direction would be arbitrary with respect to the generated structure. The distributions of all four honeycombs shown in Fig. 2(a and b) essentially coincide, implying that the selected number of Voronoi cells per structure is large enough to be considered statistically equivalent regarding these two measures. In addition, Fig. 2(c) reveals that the length and inclination of the struts are uncorrelated, further demonstrated by their Pearson correlation coefficients ranging from 0.0368 to 0.0872 for the strut length and the inclination angle of the four honeycomb structures.









2.1.4. Boundary conditions

Periodic boundary conditions are imposed and entail that fluctuations of deformation and stress vanish on average. Compression along Z is prescribed with mixed (deformation and stress) boundary conditions in the form of a volume-averaged deformation gradient tensor ($\bar{\mathbf{F}}$) and its corresponding average first Piola–Kirchhoff stress ($\bar{\mathbf{P}}$).

¹ The probability density of the strut length is $p(l) = \left[\exp\left(-\frac{(l-\mu)^2}{2\sigma^2}\right) + \exp\left(-\frac{(l+\mu)^2}{2\sigma^2}\right) \right] / (\sqrt{2\pi}\sigma)$, where μ is the average strut length, and σ is the standard deviation [19]. Above probability density integrates to a value of unity for non-negative strut lengths, since the sum of the two distributions is symmetric around $l = 0$.

Table 1

The eight crystallographic orientations considered in this study. Brass, Copper, Cube, Goss, Rotated Cube, and S orientations are typical texture components of fcc and bcc rolling textures. RZ is the orientation which is proven to be the most unstable orientation upon compression in fcc [37]. In addition, an arbitrary orientation was selected, and designated as Less symmetric. Euler angles follow Bunge's notation. Lattice unit cells are displayed in the lab coordinate system of Fig. 1.

	Euler angles/°			Miller indices		
	φ_1	ϕ	φ_2	$\parallel Z$	$\parallel X$	
Brass	35	45	0	(01 $\bar{1}$)	[2 $\bar{1}\bar{1}$]	
Copper	90	35	45	(112)	[$\bar{1}\bar{1}1$]	
Cube	0	0	0	(00 $\bar{1}$)	[100]	
Goss	0	45	0	(01 $\bar{1}$)	[100]	
Rot. cube	45	0	0	(00 $\bar{1}$)	[1 $\bar{1}0$]	
S	60	32	65			
RZ	32	85	85			
Less sym.	0	13	71			

The rigidity of the deformation boundary condition is relaxed in three steps, termed 'BC1' to 'BC3' and shown in Table 2. Only the lateral in-plane normal stress along X becomes zero in BC1. Both lateral normal stresses along X and Y are set to be zero in BC2. For BC3, essentially all but the compression normal stress component become zero.

The in-plane Young's modulus is obtained by linearly fitting the $\bar{\sigma}_{33}$ – $\bar{\epsilon}_{33}$ curve, where $\bar{\sigma}_{33}$ is the 33-component of the average CAUCHY stress tensor

$$\bar{\sigma} = \bar{\mathbf{P}}\bar{\mathbf{F}}^T / \det \bar{\mathbf{F}} \quad (1)$$

2.2. Analytical approach: uniform force or uniform strain

We follow the simplification of Gibson and Ashby [17] and Fortes and Ashby [38], i.e., we consider how a vertical force $\mathbf{f} = (00f)$ displaces the ends of an individual strut as illustrated in Fig. 3. The local x, y, z strut coordinate system is obtained by rotating the global X, Y, Z coordinate system with respect to $-Y$ (or equivalently $-y$) by $0^\circ \leq \theta \leq 180^\circ$. The compliance tensor \mathbf{S} (in Voigt notation) of a strut is defined in its local x, y, z coordinate system and, hence, will depend on the strut inclination relative to the fixed single crystal orientation of the honeycomb.

An axial force component $f \sin \theta$ results in a displacement

$$\delta_x = \frac{S_{11}l}{wt} f \sin \theta \quad (2a)$$

along the beam length, with l the length of the strut, w its width, and t its thickness. The component $f \sin \theta$ also causes a possible shear displacement

$$\delta_{z, \text{shear}} = \frac{S_{15}l}{wt} f \sin \theta \quad (2b)$$

for non-zero S_{15} component. The lateral component $f \cos \theta$, according to anisotropic beam theory [39], results in an end-to-end displacement due to bending,

$$\delta_{z, \text{bend}} = \frac{S_{11}l^3}{12I_y} f \cos \theta \quad (2c)$$

with the second moment of inertia, $I_y = w^3t/12$, being equal among all struts since w and t are constant.

The elastic work W_{el} stored in the honeycomb is taken as sum over the elastic work in each of N struts assuming the components

Download English Version:

<https://daneshyari.com/en/article/1560118>

Download Persian Version:

<https://daneshyari.com/article/1560118>

[Daneshyari.com](https://daneshyari.com)